Second-harmonic generation and parametric amplification in negative-index metamaterials

Alexander K. Popov

Department of Physics & Astronomy and Department of Chemistry, University of Wisconsin-Stevens Point, Stevens Point, WI 54481-3897

Vladimir M. Shalaev

School of Electrical and Computer Engineering, Purdue University, West Lafayette, IN 47907-2035
shalaev@purdue.edu

Abstract: Extraordinary nonlinear-optical properties originating from contra-directed wave and Poynting vectors are investigated. The feasibility of light-controlled transparency, cavityless oscillation and generation of counter-propagating entangled right- and left-handed photons is shown.

OCIS codes: 1904410, 999.9999.

1. Introduction. Metamaterials with a negative refractive index (NIMs), which are also referred to as left-handed materials (LHMs), exhibit highly unusual electromagnetic properties and promise a variety of unprecedented applications. The main emphasis in studies of NIMs has been placed so far on linear optical effects. Recently it has been shown that NIMs, which include structural elements with non-symmetric current-voltage characteristics, can possess a nonlinear magnetic response at optical frequencies [1-3] and thus combine unprecedented linear and nonlinear electromagnetic properties. The opposite directions of the wave- and Poynting vectors, which are inherent to NIMs, lead to extraordinary properties of a number of optical processes in such metamaterials. The possibility of the exact phase-matching for waves with counter-propagating energy-flows has been shown in [4] for the case of second harmonic generation (SHG) when the fundamental wave is in the negative-index frequency domain whereas the SH wave is in the positive-index domain (PID). The phase-matching of the forward and backward waves is inherent for the nonlinear optics of NIMs. Important advantages of the interaction scheme involving counter-directed Poynting vectors in the process of optical parametric amplification in conventional right-handed materials (RHMs) were discussed in early papers [5-7]. However, in RHMs such schemes impose severe limitations on frequencies of the coupled waves because one of the waves has to be in the far-infrared range, in this case.

Absorption is one of the most challenging problems that needs to be addressed for practical applications of NIMs. A transfer of the near-field image into SH frequency domain, where absorption is typically much less was proposed in [8-9], as a possible means to overcome dissipative losses and thus enable the superlens.

In this paper, we demonstrate unusual characteristics in the spatial distribution of the energy exchange between the fundamental and second-harmonic waves with counter-directed energy-flows. Both semi-infinite and finite-length NIMs are considered and compared with each other and with ordinary PIMs beyond the constant-pump approximation. The feasibility of of nonlinear-optical mirror converting 100% of the incident radiation into a reflected SH is shown. We also propose a new means of compensating losses, producing a *full transparency, or amplification, or even lasing without a cavity in NIMs*, i.e., cavity-free optical paramteric oscillation (OPO). The underlying physical mechanism is optical parametric amplification (OPA) in the field of a control electromagnetic wave with the frequency outside the negative-index domain (NID), which provides the loss-balancing OPA inside the NID. We also predict the possibility of generation of entangled pairs of counter-propagating right- and left-handed photons.

2. SHG. To demonstrate the basic properties of SHG, we consider a loss-free material, which is left-handed at the fundamental frequency ω_1 ($\epsilon_1 < 0$, $\mu_1 < 0$), whereas it is right-handed at the SH frequency $\omega_2 = 2\omega_1$ ($\epsilon_2 > 0$). We assume that an incident flow of fundamental radiation $\mathbf{S}_1$ at ω_1 propagates along the z-axis, which is normal to the surface of a metamaterial. Then the phase of the wave at ω_1 travels in the reverse direction inside the NIM [$\mathbf{k}_1$ in Fig. 1(a)]. Because of the phase-matching requirement, the generated SH radiation also travels backward with energy-flow $\mathbf{S}_2$ in the same backward direction. This is in contrast with the standard coupling geometry in a PIM [Fig. 1(b)]. Following [4], we assume that a nonlinear response is

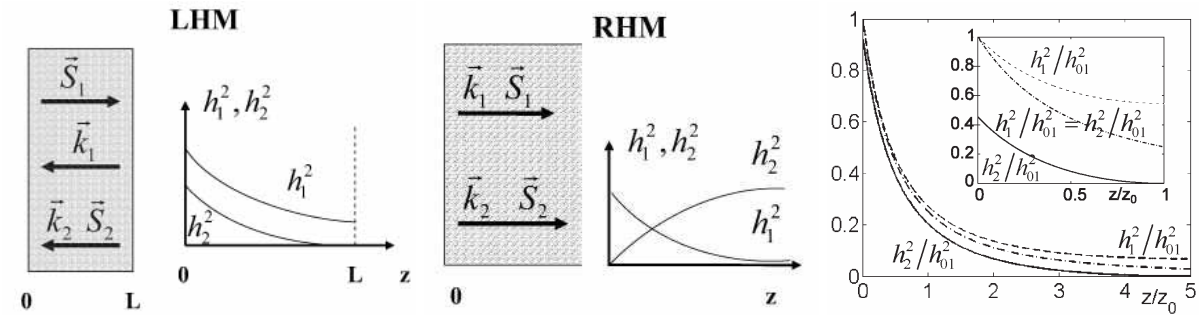

(a) **(b)** **(c)**

Fig. 1. **(a)** and **(b)**: SHG geometry and the difference between SHG in LHM and RHM loss-free slabs. **(c)**: The squared amplitudes for the fundamental wave (the dashed line) and SHG (the solid line) in a lossless NIM slab of a finite length. Inset: the slab has a length equal to one conversion length. Main plot: the slab has a length equal to five conversion lengths. The dash-dot lines show the energy-conversion for a semi-infinite NIM. (a)-(d): $\Delta k = 0$.

primarily associated with the magnetic component of the waves. The Manley-Rowe relations for the field amplitudes and for the energy-flows are given by:

$$(k_1/\epsilon_1)(dh_1^2/dz) + (k_2/2\epsilon_2)(dh_2^2/dz) = 0, \quad (dS_1/dz) - (dS_2/dz) = 0. \tag{1}$$

The latter equation accounts for the difference in the signs of ϵ_1 and ϵ_2, which brings radical changes to the spatial dependence of the field intensities discussed below. Assuming $\epsilon_1 = -\epsilon_2$ one can readily see that equation (1) predicts that the *difference* between the squared amplitudes remains constant through the sample [Fig. 1(a)], which is in striking difference with the requirement that the *sum* of the squared amplitudes is constant in the analogous case in a PIM [Fig. 1(b)]. Due to the opposite directions of $\mathbf{S}_1$ and $\mathbf{S}_2$ and, hence, the boundary conditions imposed at the opposite edges of the NIM slab, $h_1(0) = h_{10}$, $h_2(L) = 0$, the field distribution within the same distance inside the slab appears dependent on the entire slab thickness even at the exact phase matching $\Delta k = 0$ [Fig. 1(c)]. It also appeares that $h_1(z) = h_2(z)$ in a semi-infinite lossless NIM slab, and it operates as a nonlinear-optical mirror which converts 100% of fundamental beam into reflected SH [Fig. 1(c), the dash line]. *Concurrent decrease of both waves along the z-axis* and the spatial dependencies shown in Fig. 1(c) are in sharp contrast with those for the conventional process of SHG in a PIM [c.f. with Fig.1(b)].

3. Laser-induced transparency and OPO in NIMs. We now assume that a left-handed wave at ω_1 falls in a NID and travels with its wavevector $\mathbf{k}_1$ directed along the z-axis [Fig. 2(a)]. Then its energy-flow $\mathbf{S}_1$ is directed against the z-axis. We also assume that the sample is illuminated by a higher-frequency wave traveling along the axis z. The frequency of this radiation ω_3 falls in a PID. The two coupled waves with *co-directed* wavevectors $\mathbf{k}_3$ and $\mathbf{k}_1$ generate a difference-frequency idler at $\omega_2 = \omega_3 - \omega_1$, which is in a PID. The idle wave contributes back into the wave at ω_1 through three-wave coupling and thus enables OPA at ω_1 by converting the energy of the pump field at ω_3. Thus, the process under consideration involves a three-wave mixing with *all wavevectors directed* along z. Note that the energy flow of the signal wave, $\mathbf{S}_1$, is directed against z, i.e., it is directed *against* the energy flows of the two other waves, $\mathbf{S}_2$ and $\mathbf{S}_3$. Such a coupling scheme is in contrast with the conventional phase-matching scheme for OPA [Fig. 2(b)]. The Manley-Rowe relations, which follow from the Maxwell's equations at absorption indices $\alpha_1 = \alpha_2 = 0$, have the form:

$$d\left[(S_{1z}/\hbar\omega_1) - (S_{2z}/\hbar\omega_2)\right]/dz = 0, \quad d\left[\sqrt{\mu_1/\epsilon_1}(h_1^2/\omega_1) + \sqrt{\mu_2/\epsilon_2}(h_2^2/\omega_2)\right] dz = 0. \tag{2}$$

Equation (2) describes the creation of pairs of *entangled counter-propagating photons* $\hbar\omega_1$ and $\hbar\omega_2$; it takes into account the opposite signs of the corresponding derivatives with respect to z. The equation predicts that the *sum* of the terms proportional to the squared amplitudes of the signal and idler remains constant through the sample, which is in contrast with the requirement that the *difference* of such terms is constant in the case of a PIM. Equations for slowly varying amplitudes reveal unusual spatial properties for the three-wave mixing process inside a LHM [c.f., Fig. 2(c) and (d)], which depends on the product gL. Here, g is the factor proportional to the product of squared nonlinear susceptibility and the intensity of the pump field.

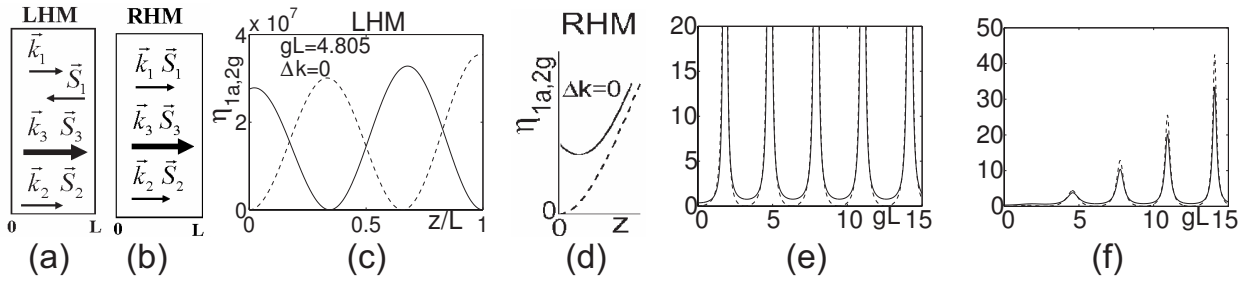

Fig. 2. (a)-(d): The difference between OPA processes in NIMs and PIMs. (a) and (b) – phase matching schemes, (c) and (d) - a typical difference in the signal (the solid line) and the idler (the dashed line) spatial intensity distributions. (e)-(f): Output amplification, η_{1a} (the solid line), and the DFG factor η_{1g} (the dashed line) for the backward wave at z=0. (e) $\Delta k = 0$. (f) $\Delta kL = \pi$. (c),(e) and (f): $\alpha_1 L = 1$, $\alpha_2 L = 1/2$.

A *strong resonance dependence of the output intensity of the left-handed wave on the factor gL* [Fig. 2(e) and (f)] indicates that unless the pump *intensity and the phase matching are appropriately optimized*, the maximum of the amplitude of the left-handed wave may occur inside rather than on the output edge of the slab [Fig. 2(c)]. The OPA can *not only fully compensate for absorption but even turn into oscillations* when the intensity of the control field reaches values given by a periodic set of increasing numbers [Fig. 2(e) and (f)].

The important advantage of the backward SHG, OPA, and OPO in NIMs investigated here is the distributed feedback, which enables oscillations without a cavity. In NIMs, each spatial point serves as a source for the generated wave in the reflected direction, whereas the phase velocities of all the three coupled waves are co-directed. For a more detailed consideration see [10].

References

1. M. Lapine, M. Gorkunov and K. H. Ringhofer, "Nonlinearity of a metamaterial arising from diode insertions into resonant conductive elements," Phys. Rev. E **67**, 065601 (2003).
2. A.A. Zharov, I.V. Shadrivov, and Yu. S. Kivshar, "Nonlinear properties of left-handed metamaterials," Phys. Rev. Lett. **91**, 037401 (2003).
3. M. Lapine and M. Gorkunov, "Three-wave coupling of microwaves in metamaterials with nonlinear resonant condactive elements," Phys. Rev. E **70**, 66601 (2004).
4. I.V. Shadrivov, A.A. Zharov and Yu. S. Kivshar, "Nonlinear left-handed metamaterials," arXiv: physics/0506092 (2005).
5. S.E. Harris, "Proposed backward wave oscillations in the infrared," Appl. Phys. Lett., **9**, 114, (1966).
6. K. I. Volyak and A. S. Gorshkov, "Investigation of parametric generator with backward wave," Radiotekhnika i Elektronika (Radiotechnics and Electronics) **18**, 2075 (1973) (Moscow, in Russian).
7. A. Yariv, *Quantum Electronics*, 2d ed., New York: Wiley, 1975, Ch. 18.
8. V.M. Agranovich, Y.R. Shen, R.H. Baughman and Zakhidov, "Linear and nonlinear wave propagation in negative refraction metamaterials," Phys. Rev. B **69**, 165112 (2004).
9. A.A. Zharov, N. A. Zharova, Il.V. Shadrivov and Yu. S. Kivshar, "Subwavelength imaging with opaque nonlinear left-handed lenses," Appl. Phys. Lett. **87**, 091104-3 (2005).
10. A. K. Popov and V.M. Shalaev, "Negative-Index Metamaterials: Second-Harmonic Generation, Manley-Rowe Relations and Parametric Amplification," http://arxiv.org/abs/physics/0601055